Title

Membrane biogenesis during B cell differentiation: most endoplasmic reticulum proteins are expressed coordinately.

Journal

Journal of Cell Biology, 110(5)

ISSN

0021-9525

Authors

Wiest, DL
Burkhardt, JK
Hester, S
et al.

Publication Date

1990-05-01

DOI

10.1083/jcb.110.5.1501

Peer reviewed

Membrane Biogenesis during B Cell Differentiation: Most Endoplasmic Reticulum Proteins Are Expressed Coordinately

David L. Wiest, Janis K. Burkhardt, Susan Hester, Michael Hortsch,* David I. Meyer,‡ and Yair Argon

Department of Microbiology and Immunology, Duke University Medical Center, Durham, North Carolina 27710; *Department of Molecular and Cell Biology, University of California, Berkeley, Berkeley, California 94720; and ‡Department of Biological Chemistry, School of Medicine, University of California, Los Angeles, Los Angeles, California 90024

Abstract. The induction of high-rate protein secretion entails increased biogenesis of secretory apparatus organelles. We examined the biogenesis of the secretory apparatus in the B cell line CH12 because it can be induced in vitro to secrete immunoglobulin (Ig). Upon stimulation with lipopolysaccharide (LPS), CH12 cells increased secretion of IgM 12-fold. This induced secretion was accompanied by preferential expansion of the ER and the Golgi complex. Three parameters of the rough ER changed: its area and volume increased 3.3- and 3.7-fold, respectively, and the density of membrane-bound ribosomes increased 3.5-fold. Similarly, the area of the Golgi stack increased 3.3-fold, and its volume increased 4.1-fold. These changes provide sufficient biosynthetic capacity to account for the increased secretory activity of CH12. Despite the large increase in IgM synthesis, and because of the expansion of the ER, the concentration of IgM within the ER changed less than twofold during the differentiation process.

During the amplification of the rough ER, the expression of resident proteins changed according to one of two patterns. The majority (75%) of rough microsomal (RM) proteins increased in proportion to the increase in rough ER size. Included in this group were both lumenal proteins such as Ig binding protein (BiP), and membrane proteins such as ribophorins I and II. In addition, the expression of a minority (~9%) of RM polypeptides increased preferentially, such that their abundance within the RM of secreting CH12 cells was increased. Thus, the expansion of ER during CH12 differentiation involves preferential increases in the abundance of a few resident proteins, superimposed upon proportional increases in most ER proteins.

MEMBRANE-bound and secreted proteins are synthesized, processed, and sorted by a series of organelles, including the ER, Golgi complex, and various transport vesicles. Regulation of the biogenesis of these organelles has not been studied extensively. In many cell types, the size of the secretory apparatus increases as its secretory workload increases. In particular, increased secretion correlates with amplification of the rough ER membranes in a wide variety of systems. When frog hepatocytes are stimulated to secrete vitellogenin with estradiol-17β, their rough ER is expanded (6, 20). A similar correlation has been observed for rat seminal vesicle cells induced by testosterone to secrete plasma proteins S and F (13), and for aleurone cells of barley induced with gibberellic acid to secrete α-amylase (5). Resting B lymphocytes can be stimulated to secrete Ig by either mitogens (12, 36, 48) or specific antigen (2, 49). In both cases the rough ER is amplified (12, 48), indicating that its amplification correlates with increased secretory activity, independent of the mode of stimulation.

The link between secretory activity and ER size is also evident during regression to the basal level. Withdrawal of estradiol from frog hepatocytes results in concomitant decreases in vitellogenin secretion and rough ER volume (6, 20). Likewise, suppression of lipopolysaccharide (LPS)[1] stimulation of B cells by treatment with anti-surface Ig inhibits both Ig secretion and expansion of the rough ER (23). All these observations indicate that high rate secretion and expansion of the ER are coupled.

The mechanisms that link ER amplification and the onset of the secretory state are yet to be addressed experimentally. Few data are available describing the changes in ER protein expression that underlie rough ER amplification. This is particularly true for those proteins that play a direct functional role in secretion.

The murine B cell line, CH12, is an excellent tool for studying the biogenesis of secretory organelles and expression of their resident proteins, because its secretory state is easily manipulated in vitro by treatment with mitogens like LPS (4, 31). The differentiation of CH12 in vitro resembles

1. *Abbreviations used in this paper*: BiP, binding protein; DAGAT, diacylglyceroltransferase; endo H, endoglycosidase H; GSBP, glycosylation site binding protein; LPS, lipopolysaccharide; RM, rough microsomal fraction.

that of normal B cells in that it is induced by its specific antigen, senescent erythrocytes, and specific T cells (31, 32). Likewise, the patterns of expression of Ig genes and cell surface proteins during CH12 differentiation also resemble those of normal, polyclonal B cells (40, 50). In this paper, we examined quantitatively the expansion of the rough ER during CH12 differentiation and we evaluated the changes in expression of resident ER proteins that underlie the amplification of this organelle.

Materials and Methods

Cell Culture

CH12 cells were passaged as an ascitic tumor in B10.A mice from our breeding colony. Upon removal from the mouse peritoneum, this population contains >94% CH12 cells (4, 31). The cells were plated at 1.3×10^5 per ml in DME (Hazelton Biologics, Lenexa, KS) supplemented as described (50), and incubated for 48 h in the presence or absence of 50 μg/ml LPS (*Escherichia coli B* [055:B5]; Difco, Detroit, MI). Differentiation of CH12 cells was evaluated by enumerating the Ig-secreting cells in the cultures. Since CH12 produces an IgM(κ) reactive with senescent erythrocytes (4), the number of secreting cells was measured by a direct plaque assay on bromelain-treated sheep erythrocytes, as described (50).

Metabolic Labeling, Immunoprecipitation, and Electrophoresis

Labeling of CH12 cells with [^{35}S]methionine (>600 Ci/mmol, Amersham Corp., Arlington Heights, IL) was done as described previously (52), at 100 μCi/ml. Cell lysis, immunoprecipitation, and digestion with endoglycosidase H (endo H) were performed as described (3). Ig was immunoprecipitated quantitatively with rabbit anti-mouse κ antiserum (Organon Teknika, Malvern, PA) and protein A-Sepharose (Sigma Chemical Co., St. Louis, MO).

Stereological Measurements

Three populations of CH12 cells were analyzed: (*a*) cells cultured with LPS (Ig-secreting cells), (*b*) cells cultured without LPS (nonsecreting cells), and (*c*) cells not cultured at all (ascitic cells). The ascitic cells served as a control for possible changes due to adaptation to culture alone. In all cases, the three populations were processed for electron microscopy in parallel, as described previously (8).

Stereological analysis was performed according to the methods of Weibel (51). Two independent stereological sets, each containing all three cell populations, were analyzed. Each set consisted of electron micrographs magnified 8,000, 27,000, 38,000, and 53,000 times (15–20 micrographs per magnification). We measured cell volume, cytoplasmic volume, and nuclear volume from 8,000× micrographs. Random sampling was assured by photographing centered grid squares while moving across the sections. The micrographs at a magnification of 27,000 were used to measure mitochondrial volume, volume of the "Golgi exclusion zone" (reference 37 and see below), membrane area of the ER and plasma membrane, and the density of bound ribosomes. Random micrographs at this magnification were generated by photographing the cell closest to one corner of each grid square. We defined the Golgi exclusion zone as the area of low electron density surrounding the Golgi stack which contains multiple vesicles, centrioles, and endosomes, but excludes mitochondria, ribosomes, and rough ER elements (37, and see Fig. 3 *c*). Micrographs magnified 38,000 times were used to measure the volume and surface area of the Golgi stack. Each of these micrographs contained a Golgi exclusion zone, randomly photographed while moving along grid bars. Micrographs magnified 53,000 times, used to measure ER volume, were generated by photographing any part of a cell visible in the field while moving along grid bars.

Estimation of Mean Cell Volume

The mean cell volume served as the reference space. It was determined by converting mean caliper diameter to cell volume, assuming that CH12 cells are spheres (51). The mean caliper diameter of an ovoid object (such as CH12) approximates the diameter of the object were it indeed spherical. It was determined by averaging the cell's maximum and minimum diameters, excluding plasma membrane projections. Since the mean caliper diameter can deviate from the true cell diameter due to shrinkage during preparation of samples, the cell diameter was also measured by an independent method. CH12 cells were passed through a fluorescence-activated cell sorter (FACS, model Ortho 50-H; Ortho Instruments, Westwood, MA), and their diameter was derived by comparing their axial light extinction to that of calibrated latex beads (38). The mean caliper diameter and the FACS-derived cell diameter are compared in Table I. For all CH12 populations examined (ascitic, unstimulated, and LPS-stimulated), the mean caliper diameter was consistently 25% smaller than the FACS-derived diameter. While the FACS-derived diameter avoids possible fixation artifacts, it overestimates the actual cell diameter, because plasma membrane projections contribute to the axial light extinction (38). Considering the inherent differences in the techniques, the two diameter measurements are in good agreement. Since all subsequent stereological measurements were made on electron micrographs, we used the cell volume measurement calculated from the mean caliper diameter as our reference space. The cell volume (V) was calculated from the mean (D) of the mean caliper diameters, according to $V = 4/3\ \pi(kD/2)^3$, where k is a factor that both incorporates magnification and corrects for sampling of a sphere (51).

Volume Measurements

The volumes of the cytoplasm, nucleus, mitochondria, Golgi exclusion zone, Golgi stack, and ER were all measured by determining the volume fraction (V_v) with a grid containing test points in linear array (1 cm spacing). V_v is equal to the number of test points falling on the structure of interest, divided by the number of points falling on the containing space (51), which in our case was the cell volume. All volume measurements were converted to absolute values by multiplying by the mean cell volume.

Because there were few Golgi stacks on randomly selected micrographs, the number of random micrographs needed to measure the stack was prohibitively large. Therefore, we first determined the V_v of the Golgi exclusion zone as described above. Then, we photographed every Golgi exclusion zone, and used these micrographs to calculate V_v of the Golgi stack within the Golgi exclusion zone.

Surface Area Measurements

Surface areas of the plasma membrane, Golgi stack, and ER were calculated by determining their surface density (S_v) and subsequently normalizing S_v to cell volume. S_v is equal to two times the number of line intersections with the membrane of interest, divided by the total length of line on the containing space (51). S_v was measured using grids of test lines with 1 cm spacing for all structures except the ER, where a grid with 2 cm spacing was used. Due to the continuity of the ER with the outer membrane of the nuclear envelope, the area of the rough ER was quantified both including and excluding the nuclear envelope. However, because the area of the nuclear envelope did not change significantly during differentiation, only the values excluding it are presented. The calculated surface area of the Golgi stack is an underestimate, since we chose to exclude grid intersections of tangentially cut Golgi membranes when we could not be certain that they were cisternal membranes. In addition, we made no attempt to quantify the vesicular elements of the Golgi complex, including the *trans*-Golgi reticulum.

Density of Bound Ribosomes

The number of ribosomes bound per unit area of rough ER membrane was calculated by determining the numerical density (N_v) of ER-bound ribosomes and then dividing it by the rough ER S_v. N_v is equal to the total

Table I. Diameter Measurements of CH12 Populations

Cell population	Mean caliper	FACS-derived
	μm	μm
Ascitic	7.19 ± 1.66 (n = 105)	10.13 ± 1.73 (n > 10,000)
Unstimulated	7.59 ± 2.07 (n = 91)	10.18 ± 1.93 (n > 10,000)
LPS stimulated	9.13 ± 2.12 (n = 74)	12.00 ± 2.25 (n > 10,000)

number of bound ribosomes in the sample, divided by the total area of the sample multiplied by the mean ribosome diameter (51). The mean ribosome diameter was measured using a reticle.

Statistical Analysis

As explained above, each of the stereological parameters (P) was estimated by multiplying its respective ratio estimate (R; that is, V_v, S_v, or N_v) by the mean cell volume (V). Therefore, the variance of P is affected by the variances of both R and V in the following way:

$$\log P = \log R + \log V.$$

Assuming that R and V are independent,

$$\mathrm{Var}(\log P) = \mathrm{var}(\log R) + \mathrm{var}(\log V).$$

From this, the variance of each parameter was estimated using the approximate variance for the function of a random variable (41):

$$\mathrm{Var}(P) = P^2[\mathrm{Var}(V)/V^2 + \mathrm{Var}(R)/R^2]$$

The variance of R was approximated by

$$\mathrm{Var}(R) = \frac{n}{(n-1)\,(\Sigma Y)^2}(\Sigma X^2 + R^2\Sigma Y^2 - 2R\Sigma XY)$$

where, X, the point count on structures of interest on each micrograph; Y, the point count on the containing space on each micrograph; R, $\Sigma X/\Sigma Y$; and n, the number of micrographs (see reference 51). The approximate variance of V was obtained, as above, for the function of a random variable (41). By incorporating into one constant (K) all the constants in the equation describing the volume of a sphere,

$$\mathrm{Var}(V) = 9K^2D^4\mathrm{Var}(D).$$

The statistical significance of measured differences between the unstimulated and LPS-stimulated populations was determined using the two-sample t test (41).

Isolation and Characterization of Rough Microsomes

CH12 cells to be fractionated were washed three times with ice-cold PBS containing 50 μg/ml cycloheximide and stored at −70°C until use. CH12 cells (2×10^9/fractionation) were thawed rapidly at 37°C, resuspended at a density of 1.2×10^8/ml in cavitation buffer (50 mM Tris pH 7.4, 25 mM KCl, 5 mM $MgCl_2$, 0.5 mM $CaCl_2$, 0.25 M sucrose, 100 U/ml Trasylol; FBA Pharmaceuticals, New York, NY), and lysed by nitrogen cavitation at 1,000 psi for 15 min. Nuclei and cellular debris were removed by centrifugation at 3,000 g for 5 min, and the rough microsomal fraction (RM) was isolated from the postnuclear supernatant using the sucrose gradient flotation method of Mechler and Vassalli (35).

The efficiency of this procedure was monitored by examining the distribution of several marker proteins (Table IV). The protein content of the fractions was determined using Peterson's modified Lowry assay (42). Equal quantities of protein from each gradient fraction were analyzed by immunoblotting, lectin blotting, and enzyme assays (see below). Lumenal contents of microsomes were monitored by immunoblotting with anti-κ light chain (Organon Teknika). Resident ER membrane proteins were similarly monitored with anti-ribophorins I and II (21), and with antibody to p73 of intracisternal type A retroviral particles (52; a generous gift of Dr. K. Leuders and Dr. E. Kuff, National Cancer Institute, Bethesda, MD). Smooth membranes (Golgi, plasma membranes, endosomes, and lysosomes) were monitored by blotting with WGA (Sigma Chemical Co.). The specificity of WGA binding was ascertained by inhibition with N-acetylglucosamine. In addition, fractionation of Golgi membranes was monitored using galactosyltransferase activity (45).

Gel Electrophoresis and Immunoblots

Equal quantities of protein from non-secreting and secreting CH12 cells were analyzed on 9–15% polyacrylamide gradient SDS gels (3) and the proteins were visualized by silver staining. Gels intended for immunoblotting were transferred to nitrocellulose (0.45 μm pore size, Vanguard International, Neptune, NJ), blocked, and probed as described (52). The antibodies were used at the following dilutions: (*a*) anti-ribophorins I and II, 1:100; (*b*) anti-BiP, hybridoma culture supernatant, and (*c*) anti-glycosylation site binding protein, 1 μg/ml (15; a kind gift of Dr. W. Lennarz). Lectin blots were performed as described (14). Autoradiograms and lectin blots were quantified by densitometry in the transmission and reflectance modes, respectively, using a densitometer (Model 620; Bio-Rad Laboratories, Richmond, CA). Exposure times for autoradiographs were varied to ensure that the signal was in the linear range.

Table II. LPS Stimulation of CH12 Immunoglobulin Synthesis and Secretion

Parameter	Unstimulated	Stimulated	Induction
Percentage of plaque forming cells	8.5 ± 0.7	67.6 ± 6.4	8.0
Incorporation into			
μ Heavy chains	8.7	46.9	5.4
κ Light chains	2.6	15.7	6.0
Secretion during chase			
μ Chains (*180 min*)	3.4	37.6	11.0
κ Chains (*180 min*)	1.0	12.5	12.5

Incorporation into Ig chains was measured by metabolically labeling cells for 10 min, resolving immunoisolated Ig by SDS-PAGE, and then scanning the autoradiograms. The increase in incorporation in three different experiments was calculated separately and then averaged. The increase in secretion was likewise calculated separately and then averaged. The OD measured for secreted κ in unstimulated cells was set as one unit.

Isolation and Quantitation of RM-associated Ribosomal RNA

20 μg of RM protein from both unstimulated and stimulated cells was denatured with 0.1% SDS, extracted twice with phenol/chloroform, and precipitated with ethanol. A series of twofold dilutions were electrophoresed on 1% agarose gels in 90 mM Tris/90 mM boric acid/2 mM EDTA, stained with ethidium bromide, and the levels of ribosomal RNA determined by densitometry.

Enzyme Assays

The galactosyltransferase assay was performed as described (45), with one unit of activity defined as that which transfers 1 pmol of galactose to ovalbumin in 30 min at 37°C (45). The diacylglycerol-acyltransferase (DAGAT) assay was performed according to "method 2" of Coleman and Bell (11), except that the diolein was solubilized in acetone instead of ethanol. The [^{3}H]palmitoyl-Coenzyme A was a generous gift from Drs. R. Hjelmstad and R. Bell (Duke University). Units of DAGAT activity are expressed as pmoles of diacylglycerol converted to triacylglycerol in 10 min at 25°C. The glutathione-insulin-transhydrogenase assay was performed as described in reference 22, with one unit of activity defined as that which degrades 1 μg of insulin to TCA-soluble fragments in 10 min at 37°C (9).

Results

LPS Induces Both Synthesis and Secretion of IgM by CH12

Stimulation of CH12 with LPS results in an 8- to 10-fold increase in the percentage of Ig-secreting cells in the culture (see reference 49 and Table II). The plaque assay does not, however, measure the change in rate or level of secretion during differentiation. To quantify these changes we used pulse–chase analysis (Table II). The synthesis of the μ and κ chains of CH12 IgM was coordinately increased sixfold by LPS stimulation, with IgM representing 10% of newly synthesized protein in secreting cells. Secretion of IgM was stimulated 12-fold. The increase in secretion was larger than the increase in synthesis because of a shift in production from the membrane-bound to the secretory form of IgM. Approximately half of the IgM produced by unstimulated cells is the membrane-bound form, while secreting cells produce pri-

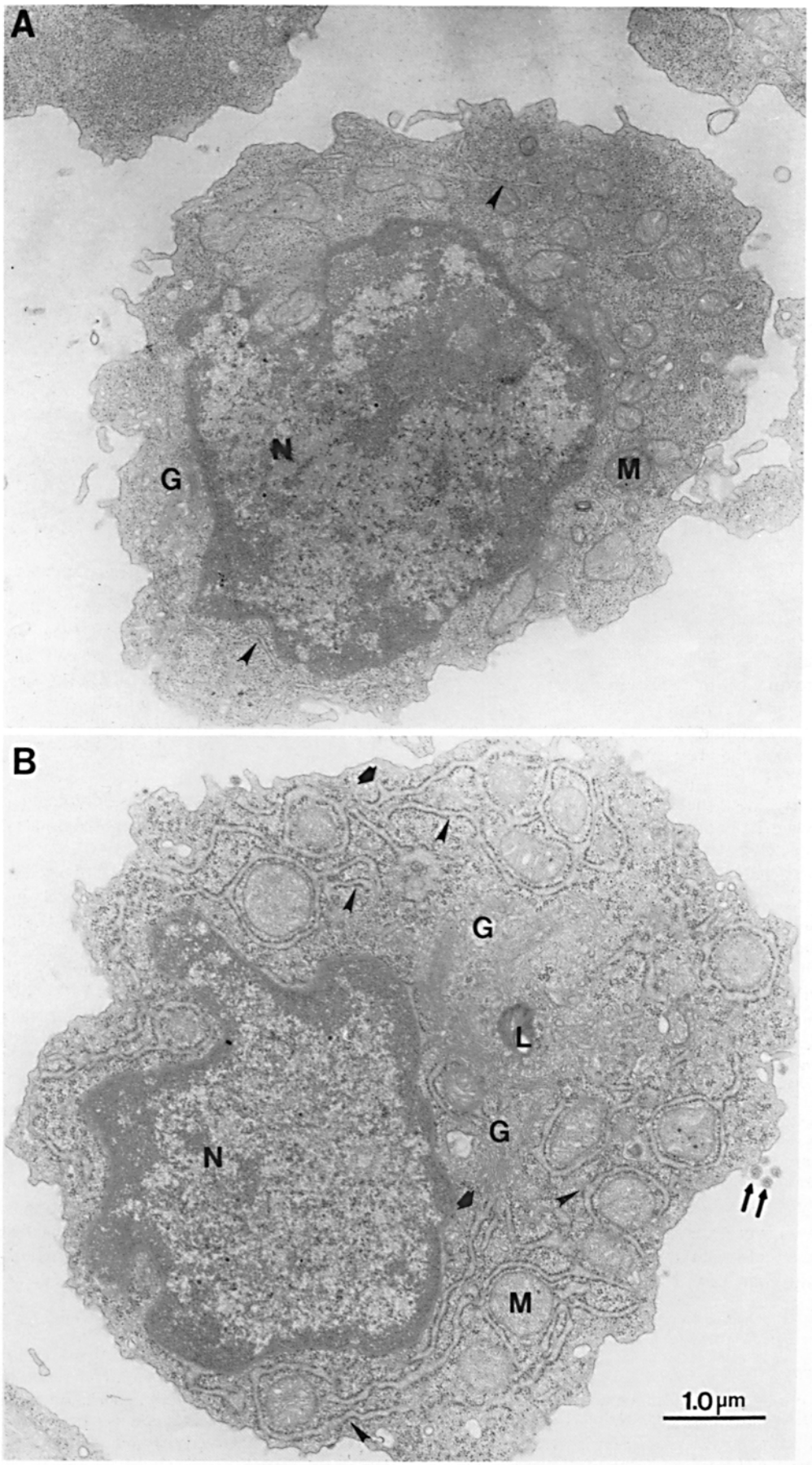
A
G
N
M
B
G
L
G
N
M
1.0 μm

marily the secretory form (50). Despite the large difference in the amount of secreted Ig, the kinetics of intracellular transport did not change. The half time for acquisition of endo H resistance remained 45 min, and the half time for IgM secretion remained 60 min (data not shown). Thus, in vitro stimulation of CH12 with LPS induced most cells in the population to become active secretors, each of them increasing dramatically the production of secretory IgM.

The ER and the Golgi Complex Are Amplified Preferentially

We next asked if the secretory apparatus of CH12 is amplified during induction of IgM secretion. Furthermore, we wanted to quantify the ultrastructural changes to provide a framework for biochemical analysis. As compared with unstimulated cells, Ig secreting CH12 were larger, possessed more cytoplasm, and displayed dramatically expanded ER and Golgi (compare Fig. 1, *a* and *b*). To quantify these and other ultrastructural differences, electron micrographs were analyzed by stereology.

The most obvious structural change was the expansion of the rough ER. Membrane area of the rough ER increased 3.3-fold, from 400 ± 51 μm^2 in nonsecreting cells to 1,318 ± 154 μm^2 in secreting cells (Fig. 2 *a*). Likewise, the volume of the rough ER increased 3.7-fold (from 10 ± 1 μm^3 to 37 ± 5 μm^3; Fig. 2 *b*), occupying 14% of the cytoplasm of LPS-stimulated cells. Visual inspection of the micrographs also revealed that the number of transitional elements of the rough ER increased approximately in proportion with the area of the organelle (Fig. 1, *broad arrows*). In addition to the increase in rough ER area and volume, there was a 3.5-fold increase in the density of ribosomes bound to the ER membrane, from 76 ± 15 to 263 ± 32 per μm^2 of ER membrane (Fig. 1 and Fig. 2, *c–d*). Since the ER membrane area increased 3.3-fold, there were 12-fold more ER bound ribosomes per LPS-stimulated CH12 cell. This provides enough translational capacity to account for the increase in Ig synthesis.

Whereas the amplification of the rough ER is dramatic, our measurements underestimate the true differences between nonsecreting and actively secreting CH12 cells. This is because both cell populations are heterogeneous with regard to Ig-secreting cell content (Tables II and III). This heterogeneity is reflected in the distribution of values for the fractional volume (V_v) of the rough ER (Fig. 3). Within the stimulated population, there are always cells whose ER V_v values fall into the typical range for unstimulated cells (Fig. 3, *open bars*). The percentage of such values corresponds well to the percentage of nonsecreting cells in the LPS-stimulated population (Tables II and III). The same correlation is seen for "contaminating" secreting cells in the unstimulated population. When values corresponding to these "contaminating" cells are subtracted from both populations, the increase in rough ER volume changes to sixfold. When

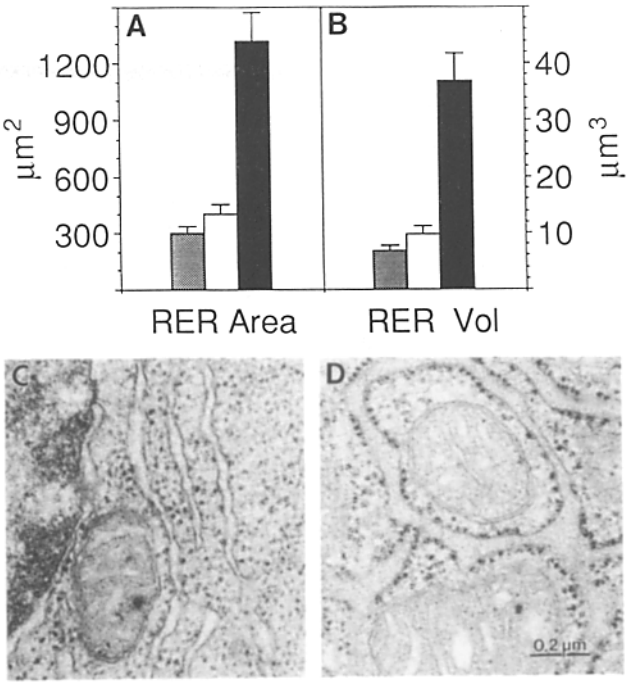

Figure 2. Stereological quantitation of rough ER amplification. Membrane area (*A*) and volume (*B*) of the rough ER were quantified from electron micrographs of CH12 cells cultured in the presence (*black bars*) or absence (*open bars*) of LPS, or not cultured at all (*hatched bars*). The differences in rough ER area and volume between the LPS-stimulated and unstimulated populations are significant ($P \leq 0.001$, two-sample *t* test). Electron micrographs of unstimulated (*C*) and stimulated (*D*) CH12 cells, illustrate the difference in density of ribosomes bound to the ER membranes.

the same correction factors are applied to other stereological parameters, their increases during CH12 differentiation also become more pronounced.

We next quantified the increase in area and volume of the Golgi stack. The membrane area of the Golgi stack increased 3.3-fold (from 32 ± 11 to 110 ± 42 μm^2 per cell) and its volume increased 4.1-fold (from 1 ± 0.3 to 4.1 ± 1.4 μm^3 per cell; Fig. 4, *a* and *b*). Interestingly, the ratio of ER volume to Golgi stack volume is a constant 10:1, both before and after CH12 differentiation. The Golgi complex includes noncisternal structures such as vesicles and the *trans*-Golgi reticulum. While we did not directly quantify the changes in these structures, we did measure the volume of the specialized "Golgi exclusion zone" which contains these structures and the Golgi stack, but excludes other organelles (Fig. 4 *c*). The volume of this zone increased from 5 ± 1.5 to 17 ± 5 μm^3 per cell during differentiation (Fig. 4 *a*). Therefore, growth of the Golgi complex involves proportional expansion of both the stack and its associated vesicle-rich area. Because the average number of cisternae per Golgi stack profile did not change (4.5 ± 1.0 in both unstimulated

Figure 1. Morphological changes during CH12 differentiation. Electron micrographs of CH12 cells cultured for 48 h in the absence (*A*) or presence (*B*) of 50 μg/ml LPS. Note the dramatically amplified rough ER in LPS-stimulated cells and the increased density of ribosomes bound to the ER membrane. *N*, nucleus; *M*, mitochondrion; *L*, lysosome; *G*, Golgi complex; *arrowheads*, rough *ER*; *thin arrows*, type C retroviruses; *broad arrows*, transitional elements of the ER.

Table III. Quantitative Analysis of CH12 Differentiation

Parameter	Ascitic	Unstimulated	Stimulated	Induction*
Cell vol (μm^3)	195 ± 17	229 ± 25	397 ± 41	1.7
Cytoplasmic vol (μm^3)	118 ± 10	140 ± 16	260 ± 28	1.9
Nuclear vol (μm^3)	77 ± 7	90 ± 11	137 ± 16	1.5
PM area (μm^2)	265 ± 27	359 ± 47	416 ± 57	1.2
Mitochondrial vol (μm^3)	10 ± 1	10 ± 2	18 ± 3	1.8
Cytoplasmic protein (10^{-5} $\mu g/cell$)	*ND*	*4.5* ± 0.05	7.0 ± 0.05	1.6
Percent secreting cells‡	5.1 ± 1.8	6.6 ± 1.0	56.4 ± 5.1	8.5

* Except for the area of the plasma membrane, the measured differences between the unstimulated and stimulated populations are statistically significant ($P \leq 0.05$).
‡ Measured by a plaque formation assay on each cell population, before fixation for EM.

and stimulated populations; $n = 50$), it follows that the Golgi complex grows either by elongating the cisternae, or by increasing the number of Golgi stacks per cell.

The amplification of the ER and Golgi complex exceeded the increase in structures not directly involved in secretion. The cell volume, cytoplasmic volume, and mitochondrial volume all increased less than twofold (Table III) with the area of the plasma membrane showing no significant change. Therefore, we conclude that the amplification of secretory organelles during CH12 differentiation is preferential.

Differentiation Is Not Accompanied by Increased IgM Concentration Within the ER

Together, the stereological measurements and the measurement of transport rates enable calculation of the flux of IgM molecules through these cells. Of particular interest was how the concentration of IgM within the ER changed after differentiation. The rate of IgM secretion by CH12 is estimated to be 180,000 $\mu_2\kappa_2$ molecules/cell/min (24). Based on the half time for acquisition of endo H resistance and the volume of the ER, we estimate the concentration of IgM in the ER of secreting cells to be 3.6 nmol/ml (0.8 mg/ml). This estimation is reasonable, because ERp99/endoplasmin, one of the most abundant ER proteins, is estimated to be 10 mg/ml in the ER (25). IgM does not comprise a large proportion of the lumenal contents of secreting cell rough ER (see Fig. 6). Because nonsecreting cells synthesize sixfold less IgM and have fourfold less ER volume, we calculate that IgM concentration in their ER is only 1.6-fold lower than in secreting cells. Therefore, even though IgM synthesis is induced considerably during differentiation, there is essentially no accumulation of IgM in the ER.

Our data also enable us to calculate the extent to which secretory IgM is concentrated during passage from the ER to the Golgi. Assuming that transit through the Golgi stack takes 10 min (from our measurement of secretion rate), the concentration of IgM molecules in the Golgi stack is 7.3 nmol/ml (1.6 mg/ml). Therefore, secretory IgM is concentrated about twofold when it moves from the ER to the Golgi. This is much less than the sevenfold concentration factor calculated for viral spike proteins in baby hamster kidney cells (17, 43). This is largely because of the differences in intracellular transport kinetics of these proteins.

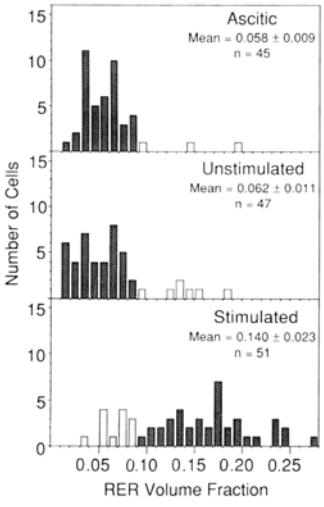

Figure 3. Histogram of rough ER volume fractions in CH12 populations. The volume fraction (V_v) of the rough ER was calculated individually for cells in each CH12 population (see Materials and Methods). Open bars in the ascitic and unstimulated populations represent V_v values within two SEM of the stimulated population. Conversely, open bars in the stimulated population represent values within two standard errors of the mean for the unstimulated population. Note that the proportion of outlying values in each distribution (ascitic, 6.7%; unstimulated, 14.9%; and stimulated, 25.5%) agrees well with the percentage of "contaminating" cells as judged by plaque formation (Tables II and III). n, number of cells analyzed in each population.

Expression of Some Known Proteins Increases in Proportion to ER Size while that of Others Is Unchanged

Given the dramatic amplification of the rough ER, we wished to examine the underlying changes in protein expression. In particular, we asked whether the ER grows by increasing all its resident proteins uniformly, or if the abundance of certain proteins increases preferentially. We therefore isolated RM fractions from both secreting and nonsecreting cells and compared their protein composition (Table IV). RM from both cell populations were substantially enriched for the integral membrane rough ER markers, ribophorins I and II (Table IV). RM protein represented ~2 and 4% of the cytoplasmic protein of nonsecreting and secreting cells, respectively ($n = 5$). Since secreting cells contained 1.6-fold more

*Table IV. Assessment of Microsomal Fractions from Secreting CH12 Cells**

Marker‡	Lysate§	Load zone	SM	RM	Enrichment‖
Protein (*mg*)	137.0	105.9	2.3	5.6	–
Kappa chain	1.5	1.0	11.1	3.8	2.5
IAP p73	2.3	0.3	5.3	22.3	9.7
Ribophorin I	4.7	1.8	6.3	24.9	5.3
Ribophorin II	2.7	1.7	2.3	13.5	5.4
WGA binding	1.8	1.4	11.5	2.7	1.5
Galactosyltransferase (*U/μg*)	2.7	1.6	13.9	7.3	2.7

* Analysis of the fractions isolated from unstimulated CH12 cells revealed a similar distribution of diagnostic markers. While the yield of RM protein was lower from unstimulated cells, enrichment for ER markers was greater, as predicted by stereology (data not shown).
‡ Unless specified otherwise, all measurements are in arbitrary OD units derived from densitometric scans of 30 μg protein per sample.
§ The fractions are: lysate, postnuclear supernatant of cavitation lysate; load zone, content of sample underlay band after centrifugation; SM, smooth microsomes; RM, rough microsomes.
‖ Specific activity in RM relative to lysate.

total cytoplasmic protein (Table III), there was roughly three-fold more RM protein per LPS-stimulated cell, in good agreement with the ER expansion measured by stereology.

Expression of specific ER proteins was examined by performing enzyme assays and immunoblots on samples from secreting and nonsecreting cells. Equal quantities of protein from cell lysates and from RM were analyzed, and the immunoreactivity of specific proteins was quantified (Table V). Ribophorins I and II are integral membrane ER proteins thought to be involved in ribosome binding (1, 27, 28, 33). BiP/GRP78 is an abundant lumenal ER protein thought to bind, among other things, Ig heavy chains until they pair with light chains (7, 18, 19). All three proteins exhibited similar expression patterns. Whereas their specific immunoreactivity was substantially higher in lysates of LPS-stimulated cells (between 3.5- and 6-fold; Fig. 5, lanes *1–2*; Table V), their immunoreactivity within the RM fraction increased only about twofold or less (Fig. 5, lanes *3–4*; Table V). In contrast to the lack of substantial change in ribophorin abundance within the RM of secreting cells, there was a fourfold increase in abundance of ribosomal RNA (Table V). This agrees well with the increased density of ER bound ribosomes measured by stereology.

The majority of the increased expression of the ribophorins and BiP can be attributed to proliferation of the ER membranes, and not increases in the concentration of these proteins within the ER. This result agrees with that predicted from both the stereology and fractionation analyses. In secreting cells the ER occupies twice as much of the cytoplasm as in nonsecreting cells. Thus, a protein which is fourfold more abundant in the cytoplasm of secreting cells should be only about twofold more abundant in isolated RM frac-

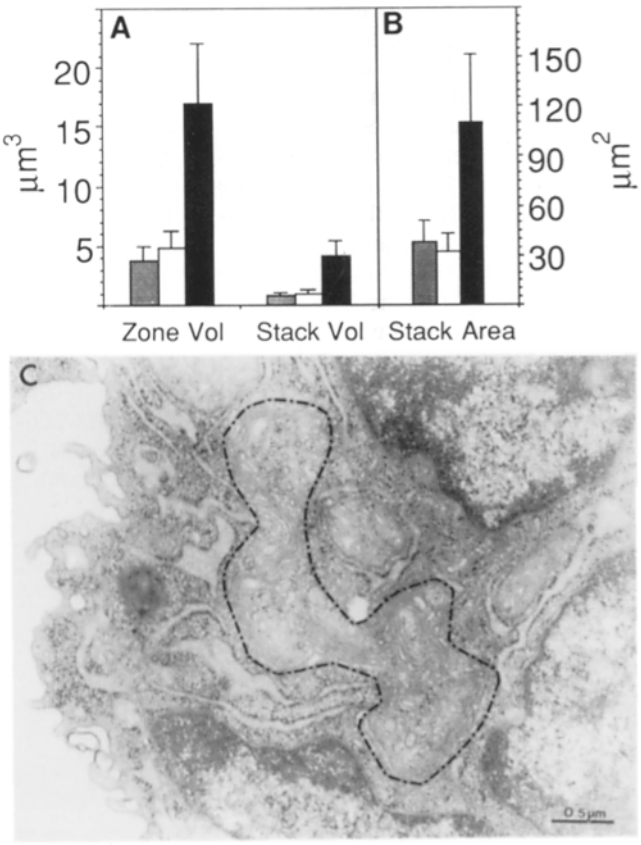

Figure 4. Stereological quantitation of Golgi amplification. The volumes of the Golgi exclusion zone and Golgi stack (*A*), as well as the membrane area of the Golgi stack (*B*) were quantified from electron micrographs of cells cultured in the presence (*black bars*) or absence (*open bars*) of LPS, and ascitic cells (*hatched bars*). The differences in estimates of Golgi parameters for the unstimulated and stimulated populations are statistically significant; Golgi zone volume ($P \leq 0.025$), Golgi stack volume ($P \leq 0.05$), and Golgi stack area ($P \leq 0.1$; *t* test). *C*, electron micrograph illustrating the Golgi exclusion zone (*broken line*).

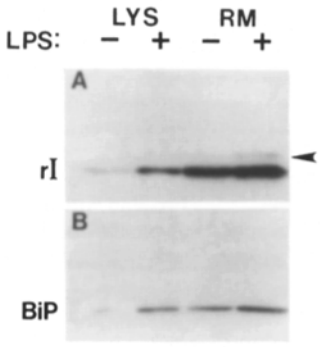

Figure 5. Immunoblot analysis of ER protein expression during differentiation. Equal quantities (30 μg) of protein from cavitation lysates (*LYS*) and purified rough microsomes (*RM*) were resolved by gel electrophoresis and blotted onto nitrocellulose. Samples from unstimulated (*–LPS*) and stimulated (*+LPS*) cells were probed with a rabbit antiserum reactive with ribophorin I (*A*), at a dilution of 1:150, or with a supernatant of an anti-BiP hybridoma (*B*). The blots were then incubated with [^{125}I]protein A, and visualized by autoradiography. *rI*, ribophorin I; *arrowhead*, p68.

Table V. Changes in Expression of Known ER Proteins during CH12 Differentiation‡*

	Lysates			Rough Membranes		
	Unstimulated	Stimulated	Induction	Unstimulated	Stimulated	Induction
Ribophorin I	1.0	4.5	4.5	16.0	27.5	1.7
Ribophorin II	0.8	2.8	3.5	11.4	15.3	1.3
Ig binding protein	1.0	6.1	6.1	7.5	16.5	2.2
28S Ribosomal RNA§	ND	ND	ND	0.8	3.3	4.1
Glycosylation site binding protein	3.2	5.4	1.7	ND	ND	0.6‖
Protein disulfide isomerase (*mU/μg*)	1.51 ± 0.10	1.42 ± 0.21	1.1	ND	ND	0.4‖
Diacylglycerol acryltransferase (*pmol/μg*)	1.40 ± 0.33	2.03 ± 0.15	1.5	ND	ND	0.6‖
P68	1.2	11.7	9.8	9.0	45.0	5.0

* All measurements, unless specified otherwise, are in arbitrary OD units generated from densitometric scans of immunoblots (30 μg protein per sample).
‡ All ratio measurements are based on multiple blots (exposures of differing durations) of samples obtained in three different experiments.
§ Generated from densitometric scans of a dilution series of ethidium bromide stained ribosomal RNA which was isolated from 30 μg of RM protein from unstimulated and stimulated CH12 cells. The linear regions of the dilution series from three experiments were compared.
‖ Extrapolated specific activity in RM.

tions. Our results regarding expression of BiP and the ribophorins agree with this prediction.

Other known ER proteins exhibited a different pattern of expression. Glycosylation site binding protein (GSBP), a lumenal protein involved in transfer of N-linked glycans to nascent polypeptides (15), was 1.7-fold more abundant in LPS-stimulated cells (Table V). Because GSBP is readily lost from microsomes during fractionation (15), it is inappropriate to measure its abundance within the RM fraction. However, using the abundance of GSBP in cell lysates it is possible to predict its abundance in RM. This calculation reveals that GSBP abundance in RM actually decreases somewhat. We also measured the changes in enzymatic activity of protein disulfide isomerase (PDI). The specific activity of PDI in CH12 lysates did not change during differentiation (Table V), so by extrapolation, its specific activity within RM actually decreases. As expected from their probable identity (16), the expression of PDI activity was consistent with that of GSBP immunoreactivity. Finally, like PDI, the activity of DAGAT, an ER enzyme involved in lipid biosynthesis (11), increased very little (1.5-fold) in cell lysates during differentiation (Table V). This indicates that, like PDI, its specific activity within the ER is slightly decreased.

In summary, when compared on a per cell basis, all the known ER proteins that we examined exhibited increases in overall expression during differentiation. However, it is more informative to note that, due to increases in cell size and rough ER content, neither these proteins nor IgM are substantially increased in abundance within the ER.

The Patterns of Expression of the Known ER Proteins Are Representative of RM Proteins in General

To determine if expression of the known ER proteins is typical of the expression of all RM proteins, we compared the total protein content of RM from nonsecreting and secreting cells. Equal quantities of protein were resolved by SDS-PAGE and visualized by silver staining. As shown in Fig. 6, the majority of polypeptides (~75%), like BiP and the ribophorins, was about equally abundant in the RM of secreting and nonsecreting cells. We did, however, reproducibly observe two groups of polypeptides whose abundance within RM did change. The first group (e.g., p101 and p60, marked by *), like GSBP and DAGAT, decreased in abundance within RM. The other group of polypeptides (e.g., p99, p73, p66, and p38, marked by arrows) was significantly increased in abundance within the RM. Therefore, the expression of this small subset of proteins (~9%) exceeded the overall increase in microsomal protein, and is preferential.

One RM protein belonging to this latter group was in fact detected in the immunoblots described above. The anti-ribophorin I antiserum used in the experiment shown in Fig.

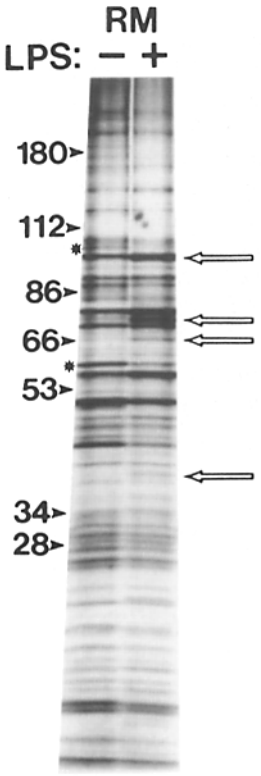

Figure 6. Expression of RM proteins during differentiation. Equal quantities of RM protein (30 μg) from unstimulated (*−LPS*) and stimulated (*+LPS*) CH12 cells were resolved by gel electrophoresis and visualized by silver staining. *Proteins that decrease in abundance during differentiation; *arrows*, proteins which increase in abundance. Apparent molecular masses (in kilodaltons) are indicated at left.

5 *a* cross-reacts with a 68-kD protein (*arrow*), which was enriched in the RM fraction. p68 was induced ~10-fold by LPS stimulation (Table V). Within RM, its abundance was increased fivefold. This magnitude of change is larger than that observed for the resident ER retroviral protein p73 (52) and for the Ig chains.

Together, these results show that the expansion of the ER during CH12 differentiation involves two major patterns of protein expression. Most ER proteins increase approximately in proportion to the size of the ER while a minority is preferentially induced.

Discussion

Our data show that LPS stimulation of the CH12 cell line results in a 12-fold increase in Ig secretion and a concomitant 3- to 4-fold preferential amplification of the ER and Golgi. In addition to the expansion of the ER, the density of bound ribosomes increases 3.5-fold, resulting in 12-fold more ribosomes which are translating membrane and secretory proteins. For the ER, the amplification is characterized by proportional increases in the expression of most resident proteins (including BiP and the ribophorins), and by preferential increases in the expression of a few proteins.

Morphological Differentiation of CH12 Resembles that of Normal B Cells

Ultrastructural changes like those that occur during CH12 differentiation have been reported for normal B lymphocytes stimulated with LPS, pokeweed mitogen, and specific antigen plus helper T lymphocytes (48, 49, 51). The only quantitative study, however, was performed by Simar on lymph node B lymphocytes stimulated in situ by injection of erythrocytes (49). He reported a tenfold increase in ER volume fraction, a larger amplification of rough ER than we report here. The difference between the two studies can be accounted for by the higher baseline measurements reported here, which are the result of the following: First, CH12, even without LPS stimulation, is already somewhat differentiated as compared to resting B cells (4, 50). Second, the baseline in Simar's in situ study necessarily includes some non-B cells, which have inherently less ER. In light of these factors, we do not consider the two sets of measurements to be significantly different. The agreement of the morphological differentiation of normal B cells and CH12 is very good, demonstrating the utility of analyzing CH12 differentiation in vitro.

Increased Ig Production Is Accommodated by Coordinate Induction of a Battery of ER Proteins

In CH12, the expansion of the ER is accompanied by an increased density of bound ribosomes. As a result, CH12 has the capacity to synthesize 12 times more membrane and secreted proteins. This is enough to account for the induction of Ig production. Because the ER volume increases, the concentration of IgM within the ER increases only about twofold, even though Ig synthesis is induced sixfold.

During expansion of the ER to produce more IgM, one might expect that resident ER proteins required for IgM synthesis and processing would be induced to a similar degree as IgM. This expectation is fulfilled for some, but not all of the proteins that we examined. Ribophorins I and II are thought to function in binding ribosomes to the ER membrane (1, 27, 28, 33), mostly because the capacity of membranes to bind ribosomes is stoichiometric with the abundance of the ribophorins (33). However, ribophorin expression in CH12 increases far less than the increase in ER-bound ribosomes. Therefore, unless there is a substantial free pool of ribophorins I and II before differentiation, we conclude that these proteins are either not needed at all, or at least not needed stoichiometrically for ribosome–membrane interactions. This is further substantiated by previous results (21). Of course, it is possible that other ER proteins which are involved in ribosome–membrane interactions, like docking protein, are limiting before differentiation. Our preliminary data suggest, however, that docking protein expression changes during differentiation even less than ribophorins. This pattern of expression is consistent with the proposed catalytic role of the docking protein (16).

Concomitantly with its synthesis, CH12 IgM is glycosylated and its folding is stabilized by intra- and interchain disulfide bonds. Since these modifications are required for IgM secretion (2, 18, 47), the enzymes responsible must be able to accommodate the increased production of IgM. Two of the modifying activities, GSBP and PDI, probably reside in the same protein (15), and one might expect that this protein would be induced. In fact, we find that the representation of GSBP within the ER actually decreases, as does PDI activity. Thus, the ratio of enzyme to substrate (IgM) is lower in secreting cells. This indicates that sufficient disulfide exchange and glycan transfer capacities must preexist to cope with the increased workload upon differentiation. Roth and Koshland have reported that PDI activity is elevated 12- to 85-fold in Ig secreting tumors, as compared to nonsecreting tumors (47). However, these authors also report that Ig secreting normal spleen cells contain only threefold more PDI than nonsecreting spleen cells. Our measurement of PDI/GSBP agrees well with their measurement in normal spleen cells, suggesting that the high concentration of PDI in various tumor lines may be associated with transformation rather than with the secretory activity of these lines.

BiP is another lumenal ER protein that is thought to be important for IgM assembly and secretion (7, 18, 19). Unlike GSBP/PDI, BiP's concentration in the ER actually rises slightly during differentiation, as does the concentration of IgM. This agrees with qualitative data showing that BiP expression is higher in Ig secreting tumors, as compared with tumors representing earlier stages in B lymphocyte differentiation (Wiest, D., unpublished observations). The correspondence between BiP expression and the accumulation of Ig within the rough ER supports the notion that BiP interacts stoichiometrically with Ig (and other proteins) during folding (19, 26).

The known proteins whose expression we examined are a very small sampling of the total resident ER proteins. The comparative analysis of total protein composition shows that the expression of most (75%) of CH12 rough ER proteins mirrors that of ribophorin I, ribophorin II, and BiP. This analysis also shows that only a few ER proteins decrease in abundance, like GSBP/PDI, or increase substantially, like p68 (see below). Thus, the overall protein composition of the ER is maintained during differentiation.

Possible Mechanisms for Regulating the Concerted Response to Secretogen

Our results show that a host of ER proteins respond in concert to the stimulation to secrete Ig. This raises two questions. First, how are so many proteins regulated coordinately? Second, what is the link between the production of a secretory product and expression of ER proteins? Several regulatory schemes can be envisioned. Perhaps, coordinate induction of many proteins results from homologous regulatory elements shared by their genes, all of which respond to the same stimulus. If so, there should be a common messenger regulating the same set of proteins in a variety of cell types in response to their respective secretory stimuli. Alternatively, the secretory product itself may secondarily regulate many ER proteins. The accumulation of the secretory product might then trigger the amplification of the ER membranes. Along these lines, Kozutsumi et al. proposed that stable association of BiP/GRP78 with misfolded proteins decreases the free pool of BiP/GRP78 in the ER lumen, and this signals induction of BiP expression (26).

Recent data provide some support for such a "feedback" model of ER regulation. Rose et al. (46) and Normington et al. (39) describe induction of the yeast homologue of BiP/GRP78, KAR2, not only under conditions which cause accumulation of misfolded proteins, but also in *sec* mutants, which accumulate properly folded secretory proteins within the ER (46). Because regulation of BiP/GRP78 in mammalian cells is at the transcriptional level (44, 10), there must be a sensor that relates the accumulation of proteins in the ER to the nucleus. BiP itself may be the putative ER sensor, however, there is no direct evidence to support this contention. We hypothesize that to fulfill the role of a sensor, this component must interact with all membrane and secreted proteins during some stage of processing. In this way it could sense an accumulation of secretory proteins, as implied by the *sec* mutants, or an increased level of translocation. The hypothesis that an increased concentration of the secretory product signals amplification of the ER predicts that at an early time in the differentiation process there is a significant accumulation of the secretory product in the ER. At later times, the concentration of the secretory product in the ER would diminish as the ER expands. In this study we examined only the endpoint of differentiation, at which time IgM concentration in the ER is only twice its concentration in non-secreting cells. Measurement of the ER concentration of IgM at an earlier time after LPS stimulation will test whether there is a transient peak in IgM concentration that could serve as a signal.

Preferential Induction of a Subset of RM Proteins

The coordinate regulation discussed above does not apply to a small percentage of RM proteins, those which are not induced and those which are upregulated significantly more than the majority. The preferentially induced proteins are particularly interesting, because among them may be proteins that are necessary for efficient intracellular transport. Preliminary characterization indicates that many of these preferentially induced proteins are integral membrane proteins (data not shown). One protein, p99, is probably equivalent to ERp99/endoplasmin (25, 29, 34). It is reported by Lewis et al. to be tenfold more abundant in post-nuclear membranes of LPS-stimulated splenic B cells (28). We see a similar induction of p99, if we correct for the differences in the methods used. Lewis et al. also reported that four other ER proteins (p49, p59, p61, and p72) are induced during spleen cell differentiation (30). The magnitude of the reported induction, however, is equal to or smaller than the change we find in BiP expression. Therefore, these proteins behave like the coordinately induced majority of ER proteins. Along with p99, we find that p68 is induced preferentially in CH12. p68 is an integral membrane glycoprotein, present in the ER of many secretory cell types (Wiest, Meyer, and Argon, manuscript in preparation). In fact, this protein was first observed in canine pancreas (21). It will be interesting to establish why proteins like p99 and p68 are induced more than most other ER components (i.e., escape coordinate regulation), and to ask what role such proteins play in secretion.

We thank Dr. D. Bole for his generous gift of mAb anti-BiP, Dr. E. Kuff and Dr. K. Leuders for the anti-p73 antiserum, and Dr. W. Lennarz for polyclonal anti-GSBP. We are indebted to Drs. A. Balber, S. Miller, and R. Bell for their helpful guidance through many parts of this work. We are particularly thankful to Dr. R. Dodge for statistical analysis of the stereological study, and to all members of the Argon lab for many critical discussions and help with this manuscript.

This work was supported by grant AI-23282 from the National Institutes of Health (NIH) and by grants from the Arthritis Foundation and the American Cancer Society. D. L. Wiest and J. K. Burkhardt were supported by NIH training grants and Y. Argon was supported by a junior faculty research award from the American Cancer Society.

Received for publication 26 September 1989 and in revised form 14 December 1989.

References

1. Amar-Costesec, A., J. A. Todd, and G. Kreibich. 1984. Segregation of the polypeptide translocation apparatus to regions of the endoplasmic reticulum containing ribophorins and ribosomes. I. Functional tests on rat liver microsomal subfractions. *J. Cell Biol.* 99:2247–2253.
2. Andersson, J., L. Lafleur, and F. Melchers. 1974. IgM in bone marrow-derived lymphocytes. Synthesis, surface deposition, turnover, and carbohydrate composition in unstimulated mouse B cells. *Eur. J. Immunol.* 4:170–180.
3. Argon, Y., and C. Milstein. 1984. Intracellular processing of membrane and secreted immunoglobulin δ-chains. *J. Immunol.* 133:1627–1634.
4. Arnold, L. W., N. C. Locasio, P. M. Lutz, C. A. Pennell, D. Klapper, and G. Haughton. 1983. Antigen-induced lymphomagenesis: identification of a murine B cell lymphoma with known antigen specificity. *J. Immunol.* 131:2064–2068.
5. Belanger, F. C., M. R. Brodl, and T-H.D. Ho. 1986. Heat shock causes destabilization of specific mRNAs and destruction of endoplasmic reticulum in barley aleurone cells. *Proc. Natl. Acad. Sci. USA.* 83:1354–1358.
6. Bergink, E. W., M. T. Tseng, and J. L. Wittliff. 1977. Sequential changes in the structure and function of hepatocytes in estrogen-treated Xenopus laevis males. *Cytobiologie.* 14:362–377.
7. Bole, D. G., L. M. Hendershot, and J. F. Kearney. 1986. Posttranslational association of immunoglobulin heavy chain binding protein with nascent heavy chains in nonsecreting and secreting hybridomas. *J. Cell Biol.* 102:1558–1566.
8. Burkhardt, J. K., S. H. Hester, and Y. Argon. 1989. The glycoprotein of VSV accumulates in a distal Golgi compartment in the presence of CCCP. *J. Cell Sci.* 92:643–654.
9. Carmichael, D. F., J. E. Morin, and J. E. Dixon. 1977. Purification and characterization of a thiol:protein disulfide oxidoreductase from bovine liver. *J. Biol. Chem.* 252:7163–7167.
10. Chang, S. C., S. K. Wooden, T. Nakaki, Y. K. Kim, A. Y. Lin, L. Kung, J. W. Attenello, and A. S. Lee. 1987. Rat gene encoding the 78-kDa glucose-regulated protein GRP78: its regulatory sequences and the effect of protein glycosylation on its expression. *Proc. Natl. Acad. Sci. USA.* 84:680–684.
11. Coleman, R., and R. M. Bell. 1976. Triacylglycerol synthesis in isolated fat cells. Studies on the microsomal diacylglycerol acyltransferase activity using ethanol-dispersed diacylglycerols. *J. Biol. Chem.* 251:4537–4543.

12. de Vreis, E., J. P. van der Weij, C. J. P. van der Veen, and A. Cats. 1983. Characterization and classification of lymphoid cells after pokeweed mitogen stimulation. *Virchows Arch. Cell. Pathol.* 43:17–30.
13. Falwell, S. E., and S. J. Higgins. 1984. Androgen regulation of specific mRNAs, endoplasmic reticulum and Golgi-system. *Mol. Cell. Endocrinol.* 37:15–27.
14. Frommel, T. O., and A. E. Balber. 1987. *Trypanosoma brucei brucei*, *T. brucei gambiense*, and *T. brucei rhodesiense*: common glycoproteins and glycoprotein oligosaccharide heterogeneity identified by lectin affinity blotting and endoglycosidase H treatment. *Exp. Parasitol.* 63:32–41.
15. Geetha-Habib, M., R. Noiva, H. A. Kaplan, and W. J. Lennarz. 1988. Glycosylation site binding protein, a component of oligosaccharyl transferase, is highly similar to three other 57 kd luminal proteins of the ER. *Cell.* 54:1053–1060.
16. Gilmore, R., and G. Blobel. 1983. Transient involvement of signal recognition particle and its receptor in the microsomal membrane prior to protein translocation. *Cell.* 35:677–685.
17. Griffiths, G., S. D. Fuller, R. Back, M. Hollinshead, S. Pfeffer, and K. Simons. 1989. The dynamic nature of the Golgi complex. *J. Cell Biol.* 108:277–279.
18. Haas, I. G., and M. Wabl. 1983. Immunoglobulin heavy chain binding protein. *Nature (Lond.).* 306:387–389.
19. Hendershot, L. M., D. Bole, G. Kohler, and J. F. Kearney. 1987. Assembly and secretion of heavy chains that do not associate posttranslationally with immunoglobulin heavy chain-binding protein. *J. Cell Biol.* 104: 761–767.
20. Herbener, G. H., R. C. Feldhoff, and M. L. Fonda. 1983. A correlated morphometric and biochemical study of estrogen-induced vitellogenesis in *Rana pipiens*. *J. Ultrastruct. Res.* 83:28–42.
21. Hortsch, M., D. Avossa, and D. I. Meyer. 1986. Characterization of secretory proteins translocation: ribosome–membrane interaction in endoplasmic reticulum. *J. Cell Biol.* 103:241–253.
22. Kaetzel, C. S., C. K. Rao, and M. E. Lamm. 1987. Protein disulfide-isomerase from human placenta and rat liver: purification and immunological characterization with monoclonal antibodies. *Biochem. J.* 241: 39–47.
23. Kearney, J. F., J. Klein, D. E. Bockman, M. D. Cooper, and A. R. Lawton. 1978. B cell differentiation induced by lipopolysaccharide. V. Suppression of plasma cell maturation by anti-μ: mode of action and characteristics of suppressed cells. *J. Immunol.* 120:158–166.
24. King, L. B., and R. B. Corley. 1989. Characterization of a presecretory phase in B-cell differentiation. *Proc. Natl. Acad. Sci. USA.* 86:2814–2818.
25. Koch, G., M. Smith, D. Macer, P. Webster, and R. Mortara. 1986. Endoplasmic reticulum contains a common, abundant calcium-binding glycoprotein, endoplasmin. *J. Cell Sci.* 86:217–232.
26. Kozutsumi, Y., M. Segal, K. Normington, M. J. Gething, and J. Sambrook. 1988. The presence of malfolded proteins in the endoplasmic reticulum signals the induction of glucose-regulated proteins. *Nature (Lond.).* 332: 462–464.
27. Kreibich, G., B. L. Ulrich, and D. D. Sabatini. 1978. Proteins of rough microsomal membranes related to ribosome binding. I. Identification of ribophorins I and II, membrane proteins characteristic of rough microsomes. *J. Cell Biol.* 77:464–487.
28. Kreibich, G., C. M. Freienstein, B. N. Pereyra, B. L. Ulrich, and D. D. Sabatini. 1978. Proteins of rough microsomal membranes related to ribosome binding. II. Cross-linking of bound ribosomes to specific membrane proteins exposed at the binding sites. *J. Cell Biol.* 77:488–506.
29. Lewis, M. J., R. A. Mazzarella, and M. Green. 1985. Structure and assembly of the endoplasmic reticulum. The synthesis of three major endoplasmic reticulum proteins during lipopolysaccharide-induced differentiation of murine lymphocytes. *J. Biol. Chem.* 260:3050–3057.
30. Lewis, M. J., R. A. Mazzarella, and M. Green. 1986. Structure and assembly of the endoplasmic reticulum: biosynthesis and intracellular sorting of ERp61, ERp59, and ERp49, three protein components of murine endoplasmic reticulum. *Arch. Biochem. Biophys.* 245:389–403.
31. LoCasio, N. J., L. W. Arnold, R. B. Corley, and G. Haughton. 1984. Induced differentiation of a B cell lymphoma with known antigen specificity. *J. Mol. Cell. Immunol.* 1:177–187.
32. LoCasio, N. J., G. Haughton, L. W. Arnold, and R. B. Corley. 1984. Role of cell surface immunoglobulin in B-lymphocyte activation. *Proc. Natl. Acad. Sci. USA.* 81:2466–2469.
33. Marcantonio, E. E., A. Amar-Costesec, and G. Kreibich. 1984. Segregation of the polypeptide translocation apparatus to regions of the endoplasmic reticulum containing ribophorins and ribosomes. II. Rat liver microsomal subfractions contain equimolar amounts of ribophorins and ribosomes. *J. Cell Biol.* 99:2254–2259.
34. Mazzarella, R. A., and M. Green. 1987. ERp99, an abundant, conserved glycoprotein of the endoplasmic reticulum, is homologous to the 90-kDa heat shock protein (hsp90) and the 94-kDa glucose regulated protein (GRP94). *J. Biol. Chem.* 262:8875–8883.
35. Mechler, B., and P. Vassalli. 1975. Membrane-bound ribosomes of myeloma cells I. Preparation of free and membrane-bound ribosomal fractions. Assessment of the methods and properties of the ribosomes. *J. Cell Biol.* 67:1–15.
36. Melchers, F., and J. Anderson. 1974. IgM in bone marrow-derived lymphocytes. Changes in synthesis, turnover, and in numbers of molecules on the surface of B cells after mitogenic stimulation. *Eur. J. Immunol.* 4:181–188.
37. Mollenhauer, H. H., and D. J. Morre. 1978. Structural compartmentation of the cytosol: zones of exclusion, zones of adhesion, cytoskeletal and intercisternal elements. *Subcell. Biochem.* 5:327–359.
38. Monroe, J. G., W. L. Havran, and J. C. Cambier. 1982. Enrichment of viable lymphocytes in defined cycle phases by sorting on the basis of pulse width of axial light extinction. *Cytometry.* 3:24–27.
39. Normington, K., K. Kohno, Y. Kozutsumi, M. J. Gething, and J. Sambrook. 1989. *S. cerevisiae* encodes an essential protein homologous in sequence and function to mammalian BiP. *Cell.* 57:1223–1236.
40. Ovnic, M., and R. B. Corley. 1987. Quantitation of cell surface molecules on a differentiating, Ly-1$^+$ B cell lymphoma. *J. Immunol.* 138:3075–3082.
41. Papoulis, A. 1965. Random Variables, and Stochastic Processes. McGraw-Hill Book Co., New York. 151–152.
42. Peterson, G. L. 1977. A simplification of the protein assay method of Lowry et al., which is more generally applicable. *Anal. Biochem.* 83: 346–356.
43. Quinn, P., G. Griffiths, and G. Warren. 1984. Density of newly synthesized plasma membrane proteins in intracellular membranes II. Biochemical studies. *J. Cell Biol.* 98:2142–2147.
44. Resendez, E., Jr., J. Ting, K. S. Kim, S. K. Wooden, and A. S. Lee. 1986. Calcium ionophore A23187 as a regulator of gene expression in mammalian cells. *J. Cell Biol.* 103:2145–2152.
45. Rome, L. H., A. J. Garvin, M. M. Allietta, and E. F. Neufeld. 1979. Two species of lysosomal organelles in cultured human fibroblasts. *Cell.* 17:143–153.
46. Rose, M. D., L. M. Misra, and J. P. Vogel. 1989. KAR2, a karyogamy gene, is the yeast homolog of the mammalian BiP/GRP78 gene. *Cell.* 57:1211–1221.
47. Roth, R. A., and M. E. Koshland. 1981. Role of disulfide interchange enzyme in immunoglobulin synthesis. *Biochemistry.* 20:6594–6599.
48. Shohat, M., G. Janossy, and R. R. Dourmashkin. 1973. Development of rough endoplasmic reticulum in mouse splenic lymphocytes stimulated by mitogens. *Eur. J. Immunol.* 3:680–687.
49. Simar, J. L. 1975. Analyse stéreologique de la différenciation des cellules immunitaires ganglionnaires au cours des réactions du type humoral. *Pathol. Biol.* 23:444–447.
50. Stockdale, A. M., J. L. Dul, D. L. Wiest, M. Digel, and Y. Argon. 1987. The expression of membrane and secreted immunoglobulin during the in vitro differentiation of the murine B cell lymphoma CH12. *J. Immunol.* 139:3527–3535.
51. Weibel, E. R. 1979. Stereological Methods. I. Practical Methods for Biological Morphometry. Academic Press, Inc., London. 1–185.
52. Wiest, D. L., J. K. Burkhardt, A. M. Stockdale, and Y. Argon. 1989. Expression of intracisternal A-type particles is increased when a B-cell lymphoma differentiates into an immunoglobulin-secreting cell. *J. Virol.* 63:659–668.